Journal of Power Technologies 100 (2) (2020) 120–128

Shunt Active Power Filter Employing Robust Extended Complex Kalman Filter based Linear Quadratic Regulator Control Strategy for Power Quality Enhancement

Rajesh Kumar Patjoshi *, Rakhee Panigrahi †

Abstract

In this paper, a new reference current generation method is proposed for effective harmonics mitigation and reactive power compensation of three-phase shunt active power filter (SAPF) under grid perturbations. The proposed reference technique is specified as a self-regulator of dc-capacitor voltage. In operation, the proposed algorithm estimates the source reference current rapidly and adaptively through power system disruptions arising at source as well as load sides. The proposed technique employs the Robust Extended Complex Kalman filter (RECKF) algorithm to generate reference current, which confirms in phase action of SAPF with the functional power system, without being reliant upon any phase-locked loop (PLL) elements or proportional integral (PI) controller loop. As a consequence, an economical SAPF system can be designed. Moreover, a Linear Quadratic Regulator (LQR) is formulated using RECKF methodology for delivering stability and robustness in the SAPF system. The design model and efficacy of the proposed algorithm are fully studied and assessed in a laboratory prototype employing dSPACE1104 to justify feasibility. The encouraging outcomes obtained experimentally demonstrate the efficiency of the proposed approach under both steady and dynamic conditions of the power system.

Keywords: Shunt active power filter, Robust extended complex Kalman filter, Linear quadratic regulator, grid perturbations

Introduction

Abnormal current harmonics in power distribution systems produced by widespread use of nonlinear loads is a major power quality problem [1]; [2] attracting huge research interest. The existence of harmonic currents in the power system not only impacts whole system efficiency, but also triggers other related problems such as overheating of equipment, failures of sensitive devices and capacitor blowing. Consequently, mitigating appliances need to be installed to limit and remove harmonic currents created by nonlinear loads. In fact, several new techniques have been suggested in the literature review [3], [4],[5] to reduce the influences of harmonic currents and the main research mechanisms have been accompanied with control algorithm proposals. SAPF is an operational mitigation device which has been widely applied to alleviate current harmonics problems. The efficacy of SAPF in current harmonics alleviation is firmly dependent upon the accuracy of its reference current creation algorithm. By having a precise reference current, the SAPF should be able to efficiently lessen harmonic problems. Although numerous methods with distinctive qualities have been proposed for producing reference current [6], [7], time domain approaches especially synchronous reference frame (SRF) and instantaneous power (pq) theory [8], [9] are still the principal methods used, owing to their simple operational features which decrease controller complication and facilitate the process for real-time implementation. Other reference current generation techniques including extraction of fundamental component have already been developed through sliding DFT, wavelet transforms etc.[10], [11]. However, their computational load is very high and are more appropriate for power quality monitoring process than for real-time uses. Further, several Kalman filtering methodologies such as Extended Kalman Filter (EKF) and Extended Complex Kalman Filter (ECKF) [12], [13], [14],[15] have been developed to accurately estimate the amplitude, phase and frequency of a noisy signal, which give rise to reference signal. RECKF is suggested in this paper, with a novel weighting function to factor in non-ideal situations such as voltage disruption, measurement noise. This weighting function is termed robust exponential function and includes the square value of the residual vector. As the residual vector increases, the effects of irregularity rapidly decrease compared to the exponential function stated formerly in [12] and therefore the suggested RECKF methodology offers enhanced estimation independent of all grid disturbances. Central to attaining proficient SAPF

*National Institute of Science and Technology, Berhampur India e-mail

†Biju Patnaik University of Technology, Parala Maharaja Engineering College Berhampur, India e-mail

operation is appropriate choice of a current controller in addition to reference generation under consideration of all grid perturbations. Over the past few decades a considerable amount of research has been carried out into structural control applications and optimal control theory. However, an optimum filtering theory is needed to gain evidence for harmonics deletion, harmonics and displacement power factor rectification, harmonics and unbalance compensation and harmonics with unbalance and displacement power factor correction. LQR has been repeatedly chosen for numerous applications[16],[17],[18] where an optimal controller is demanded. To fulfill performance criteria, LQR is implemented with appropriate state weighting matrices. The current controller involves sliding mode control, dead beat control and hysteresis current control accompanied with outer voltage regulation loop controlled by simple Proportional Integral (PI) in the SAPF system. However, LQR does not need any outward PI controller loop and seeks to minimize the performance index, which can decrease the control attempts or maintain the energy of state variables under control. A comparative assessment of both linear and nonlinear KF algorithms (KF and proposed RECKF) is performed for reference generation and also for estimation of point of common coupling (PCC) state space variables needed for designing the LQR. To validate the performance of the presented system, the design and modeling of the proposed system are carried out in a developed prototype employing dSPACE1104.

Proposed RECKF and LQR Based SAPF

Fig. 1 depicts the structure of the SAPF system. The SAPF is organized to inject current into the PCC V_{abc} so as to compensate the harmonic content of load current i_{Labc}. The grid perturbations such as measurement noise and voltage distortion at PCC are taken into account for SAPF compensation. Estimation of in-phase and in-quadrature fundamental components of both PCC voltages and load currents is done with the help of KF and the proposed RECKF.

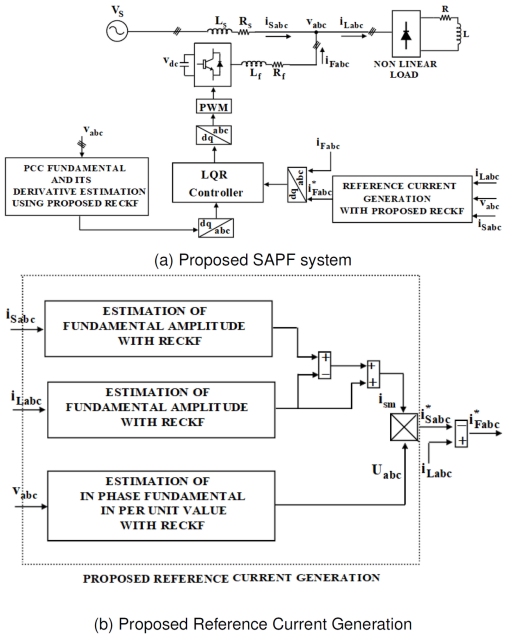

Figure 1: SAPF structure and reference generation technique

Model of Shunt Active Power Filter

The complete SAPF model in the frame is represented by equations 1, 2, 4 and 5, where i_d , i_q and v_d, v_q symbolize the frame model for filter current and PCC voltages respectively: the switching function, angular frequency of the grid, the dc linkage capacitor voltage and L_f , R_f are filter impedances.

$$[\dot{i}_{dq} = Ai_{dq} + Bd_{dq} + Ev] \tag{1}$$

$$[y_{dq} = Ci_{dq}] \tag{2}$$

where

$$A = -\begin{bmatrix} \frac{R_f}{L_f} & -\omega \\ \omega & \frac{R_f}{L_f} \end{bmatrix}, B = -\begin{bmatrix} \frac{v_{dc}}{L_f} & 0 \\ 0 & \frac{v_{dc}}{L_f} \end{bmatrix}$$
$$E = \begin{bmatrix} \frac{1}{L_f} & 0 \\ 0 & \frac{1}{L_f} \end{bmatrix}, \quad C = \begin{bmatrix} 1 & 0 \\ 0 & 1 \end{bmatrix} \tag{3}$$

$$\begin{bmatrix} \dot{i}_d \\ i_q \\ v_d \\ v_q \\ \dot{v}_d \\ \dot{v}_q \end{bmatrix} = \bar{A} \begin{bmatrix} i_d \\ i_q \\ v_d \\ v_q \\ \dot{v}_d \\ \dot{v}_q \end{bmatrix} + \bar{B} \begin{bmatrix} d_d \\ d_q \end{bmatrix} \tag{4}$$

$$y_{dq} = \bar{C} \begin{bmatrix} i_d \\ i_q \\ v_d \\ v_q \\ \dot{v}_d \\ \dot{v}_q \end{bmatrix} \tag{5}$$

$$\bar{A} = \begin{bmatrix} -\frac{R_f}{L_f} & \omega & \frac{1}{L_f} & 0 & 0 & 0 \\ -\omega & -\frac{R_f}{L_f} & 0 & \frac{1}{L_f} & 0 & 0 \\ 0 & 0 & 0 & 0 & 1 & 0 \\ 0 & 0 & 0 & 0 & 0 & 1 \\ 0 & 0 & -\omega^2 & 0 & 0 & \omega \\ 0 & 0 & 0 & -\omega^2 & -\omega & 0 \end{bmatrix}$$

$$\bar{B} = - \begin{bmatrix} \frac{v_{dc}}{L_f} & 0 \\ 0 & \frac{v_{dc}}{L_f} \\ 0 & 0 \\ 0 & 0 \\ 0 & 0 \\ 0 & 0 \end{bmatrix}, \bar{C} = \begin{bmatrix} 1 & 0 & 0 & 0 & 0 & 0 \\ 0 & 1 & 0 & 0 & 0 & 0 \end{bmatrix} \tag{6}$$

LQR Control Methodology

The benefit of LQR above over previous controllers such as hysteresis, sliding mode and dead beat controller is that it is organized to minimize the performance index, which maintains the energy of state variables under control. The plant model for LQR is defined below.

$$x_{k+1} = A_L x_k + B_L u_k \tag{7}$$

$$y_k = C_L x_k \tag{8}$$

where

$$A_L = e^{AT_s}, B_L = A^{-1}(e^{AT_s} - 1)B$$

and

$$C_L = C$$

The LQR law $u_k = -Kx_k$ minimizes the cost function,

$$J = \frac{1}{2} \sum_{k=0}^{\infty} \{x_k^T Q x_k + u_k^T R u_k\} \tag{9}$$

Q and R are the state and control weighting matrices. Gains K can be obtained through solutions of the algebraic Riccati equation.

$$P = A_L^T P (A_L - B_L K) + Q \tag{10}$$

$$K = (B_L^T P B_L + R)^{-1} B_L^T P A_L \tag{11}$$

The gain vector K is computed by the model stated in equation 4. The servo system structure is displayed in Fig. 2. The state variables associated with the PCC and the current references are estimated with KF and proposed RECKF algorithms.

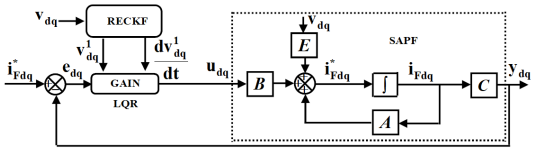

Figure 2: Control structure of LQR servo system

Estimation of the PCC Fundamental and Its Derivative

Information regarding voltages at the PCC and their derivatives is desired from the SAPF model described in Section . Assuming that the voltage at the PCC is predominant at the fundamental frequency, the resultant in-phase and in-quadrature components can be achieved through KF and the proposed RECKF. It is possible to get the subsequent relations for the fundamental component of voltage at the PCC v_{j1_k} and their corresponding derivatives $\dot{v}_{j1_k}$ that denote the state variables of the mathematical model.

$$v_{j1_k} = A_{v_{j1_k}} \sin(k\omega T_s + \theta_{v_{j1_k}}) \tag{12}$$

$$\dot{v}_{j1_k} = \omega \hat{v}^{\perp}_{j1_k} = \omega A_{v_{j1_k}} \cos(k\omega T_s + \theta_{v_{j1_k}}) \tag{13}$$

where $A_{v_{j1_k}}, \theta_{v_{j1_k}}$ are the amplitude and phase of the fundamental component of PCC voltage at the instant k, T_s is the sampling time, j represents the phase and v_{j1_k} , $v^{\perp}{}_{j1_k}$ are the in-phase and in-quadrature components respectively.

Signal formulation for Kalman filter

A single sinusoid linear signal is signified by

$$z_k = A_{v_{j1_k}} \sin(k\omega T_s + \theta_{v_{j1_k}}) \tag{14}$$

$$\omega = 2\pi f \tag{15}$$

Signal z_{k+1} can be stated as

$$z_{k+1} = x_{1_{k+1}} = x_{1_k} \cos(k\omega T_s) + x_{2_k} \sin(k\omega T_s) \tag{16}$$

$$x_{2_{k+1=}} - x_{1_k} \sin(k\omega T_s) + x_{2_k} \cos(k\omega T_s) \tag{17}$$

where x_{2_k} and x_{1_k} are denoted as

$$x_{1_k} = A_{v_{j1_k}} \sin(k\omega T_s + \theta_{v_{j1_k}}) \tag{18a}$$

$$x_{2_k} = A_{v_{j1_k}} \cos(k\omega T_s + \theta_{v_{j1_k}}) \tag{18b}$$

Signal formulation for Proposed Robust Extended Complex Kalman Filter

The signal model and filter formulations in the proposed RECKF are similar to those in ECKF [12]. The simplification modification is in the measurement error covariance matrix R_k, which is the inverse of the weighting W_k, i.e.

$$R_k = W_k^{-1} \tag{19}$$

$$W_k = W_{k-1} e^{-(y_k - H_k \tilde{x}_k)^2} \tag{20}$$

When any grid disorders happen at the PCC, the innovation vector $(y_k - H_k\tilde{x}_k)$ rises more rapidly due to the insertion of a 'square term' in the proposed exponential function $e^{-(y_k - H_k\,\tilde{x}_k)^2}$. Therefore, the amount of proposed robust exponential function decreases sooner and lastly a rapid decrease in weighting and alleviation of error can be accomplished.

Proposed Reference Current Generation Approach

Fig. 1b represents the proposed reference current generation approach, where the reference source current i^*_{Sabc} is produced by modulation of i_{sm} with the estimated in phase fundamental component of PCC voltage in p.u. value (U_{abc}) as displayed in equation 21. i_{sm} is identified as the desired peak value of source current. The importance behind this reference generation approach is evasion from the external PI controller loop, hence turning out to be a self-controller of dc-linkage voltage. The reference compensating currents i^*_{Fabc} is obtained from the equation 22.

$$i^*_{Sabc} = i_{sm} \times U_{abc} \tag{21}$$

$$i^*_{Fabc} = i_{Labc} - i^*_{Sabc} \tag{22}$$

Table 1: Experimental Parameters

Serial No.	Components	Parameters	Values
1.	SAPF	DC-link voltage	220 V
		Dc-link capacitor	2350 μF
		Filter inductor	2.5 mH
		Switching Freq.	12.5 kHz
2.	Nonlinear Load	Three Phase diode bridge Rectifier	
		Load Impedance	20 Ω, 10 mH
3.	AC source	Line–line RMS voltage	100 V
		Supply frequency	50 Hz

Result and Discussion

The performance of RECKF and LQR based SAPF system was evaluated on an experimental prototype developed in the laboratory. The nonlinear load consists of a three phase diode bridge rectifier with resistive-inductive load. A dSPACE1104 rapid prototyping controller is used to control the prototype. A four-channel digital storage oscilloscope is used to capture the waveforms during steady and dynamic conditions. Table 1 provides the full experimental system parameters and ratings. The filtered error covariance matrix was selected to be diagonal with the value of 10 pu^2. The measurement error covariance matrix and process error covariance matrix were selected to be 1.0 pu^2 and 0.0001 pu^2 respectively. The choice of Q and R matrix in LQR development was based on the performance specifications and an amount of trial and error was involved to obtain satisfactory outcomes.

Performance of the SAPF system during Steady State Condition:

Steady state SAPF system capability in harmonics compensation and reference current tracking was evaluated under normal balanced supply voltage conditions. The steady state waveforms of the SAPF system are shown in Fig. 3 and 4. The reference tracking performance of compensating current for KF-LQR and proposed RECKF-LQR are displayed in Fig. 3 and an excellent performance of the proposed method without any tracking delay was observed. Fig. 4a shows

Table 2: Harmonics Compensation Results

Test Condition	Methods of SAPF	THD (%) of phase-a source current compensation	
		Before	After
Steady State	KF-LQR	22.4 %	3.7 %
	Proposed RECKF-LQR	22.4 %	2.8 %
Dynamic State			
	KF-LQR	26.9 %	4.8 %
	Proposed RECKF-LQR	26.9 %	3.4 %

the 3-phase load currents and Fig. 4c depicts the 3-phase supply currents (= 6.30A) that are sinusoidal in the proposed method, but some distortions are seen in the KF-LQR approach (Fig. 4b). The harmonics spectra were recorded using a power quality analyzer and the harmonics spectra for phase-a load and phase-a source current are set out in Fig. 5. It can be observed that the THD in the load current is 22.4 % and the THD of the source current dropped to 3.7 % and 2.8 % in the case of KF-LQR and the proposed approach respectively. As a result, the proposed approach affords improved reduction in % of THD as per IEEE519 measure.

Performance of the SAPF system during Dynamic Load Condition

The dynamic performance of the SAPF system is evaluated by subjecting the load change from (R, L=30 Ω and 15 mH) to (R, L=20 Ω and 10 mH) (Fig. 6a). The source current profiles for both KF-LQR and the proposed approach are shown in Fig. 6b and 6c. As seen, the proposed SAPF exhibits better response compared to KF-LQR. Also, the capacitor voltage (Fig. 6d) is quickly settled at its reference in the case of the proposed SAPF system even under dynamic conditions. Fig. 7 shows that the THD of source current was successfully lowered from 26.9 % to 4.8 % and 3.4 % in KF-LQR and the proposed approach respectively. Hence, the proposed approach has superior steady-state and dynamic performance, which is clearly evident from the harmonics compensation outcomes demonstrated in Table 2.

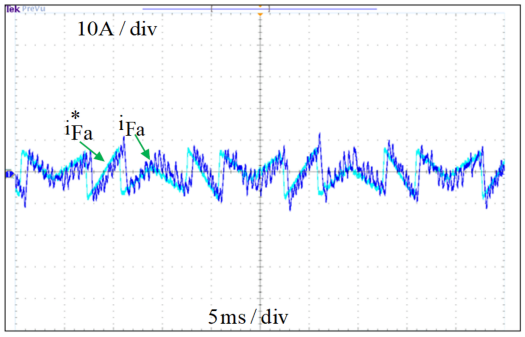

(a) KF-LQR-SAPF

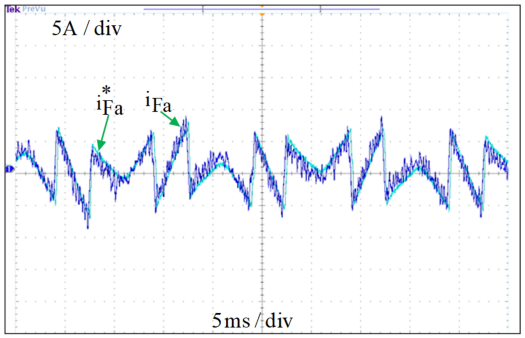

(b) Proposed RECKF-LQR-SAPF

Figure 3: Tracking Performance of Compensating Current

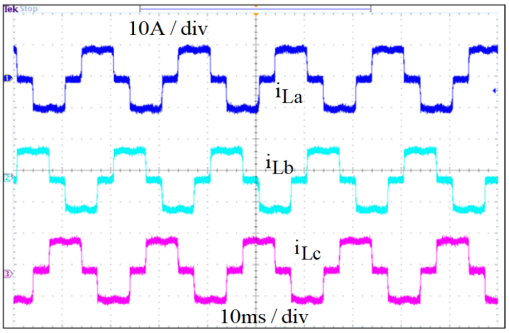

(a) 3-phase Load currents

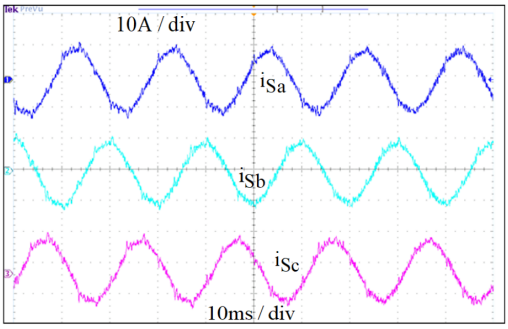

(b) 3-phase Source currents in KF-LQR-SAPF

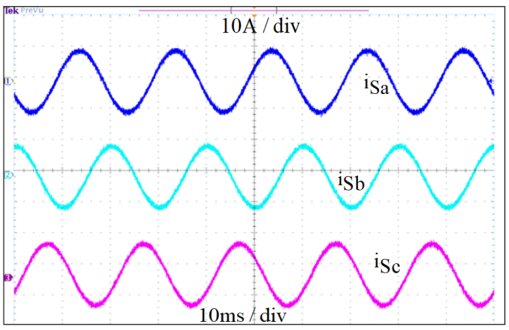

(c) 3-phase Source currents in Proposed RECKF-LQR-SAPF

Figure 4: Steady State Current of SAPF

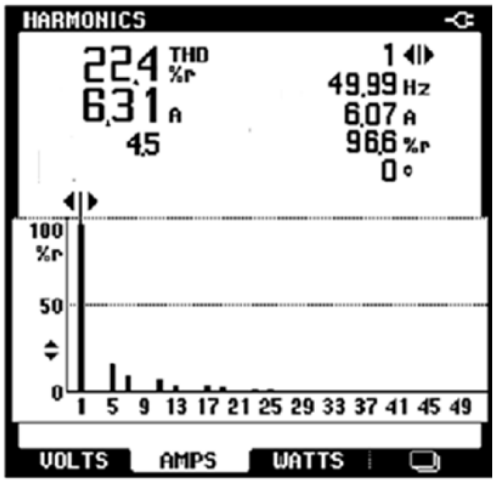

(a) phase-a load current

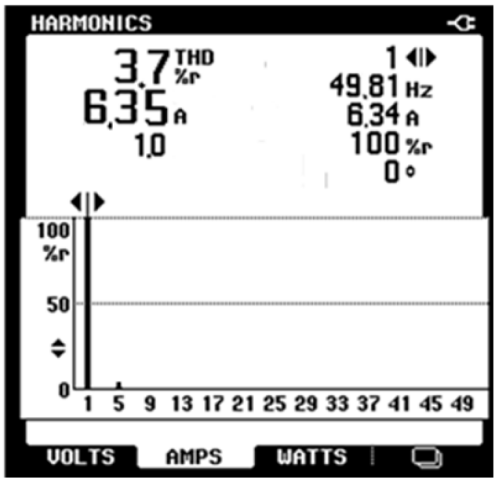

(b) phase-a source current in KF- LQR-SAPF

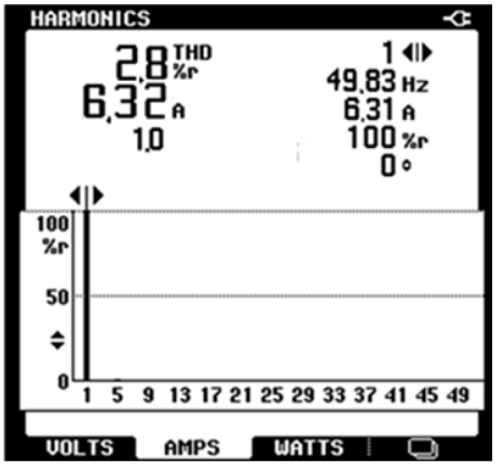

(c) phase-a source current in Proposed RECKF-LQR-SAPF

Figure 5: Steady State: Spectra analysis

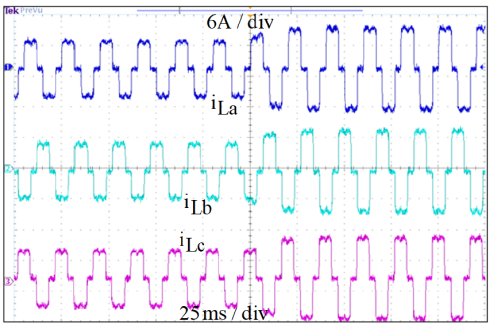

(a) 3-phase Load currents

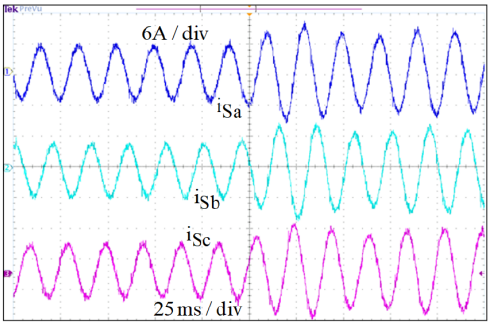

(b) 3-phase Source currents in KF-LQR-SAPF

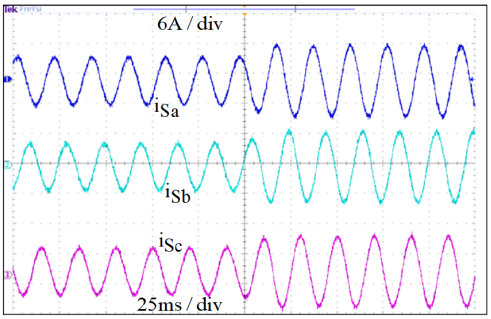

(c) 3-phase Source currents in Proposed RECKF-LQR-SAPF

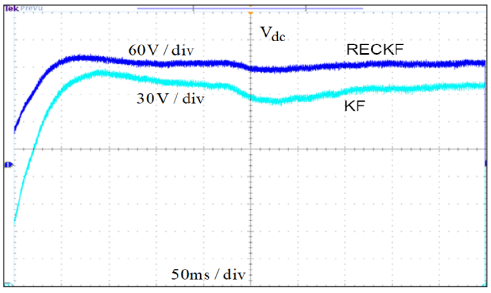

(d) dc-link capacitor voltage for KF-LQR-SAPF and Proposed RECKF-LQR-SAPF

Figure 6: Dynamic State performance of SAPF

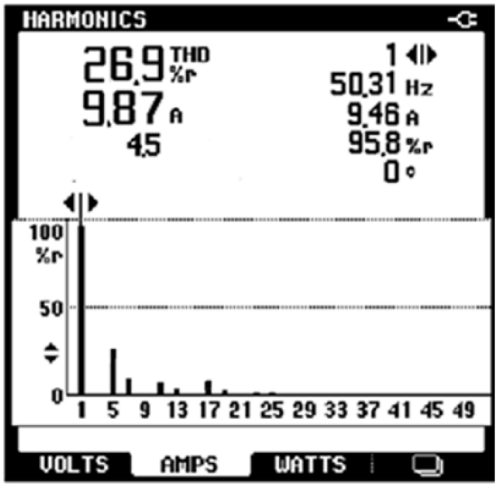

(a) phase-a load current

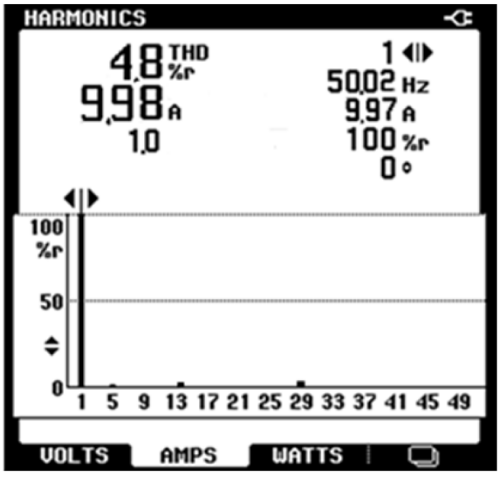

(b) phase-a source current in KF-LQR-SAPF

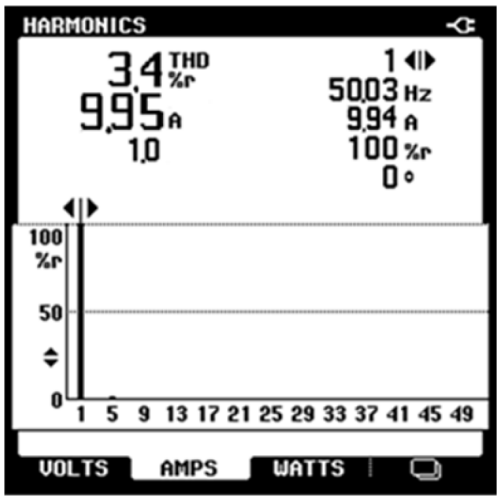

(c) phase-a source current in Proposed RECKF-LQR-SAPF

Figure 7: Dynamic State: Spectra analysis

Conclusions

The performance of the proposed RECKF-LQR based SAPF system under both steady state and dynamic conditions has been analyzed in detail. This technique self regulates the dc linkage voltage without any external PI controller loop or any PLL. The proposed RECKF algorithm produces accurate references for the LQR under grid disturbances such as voltage alteration, phase angle jump, frequency deviancy and measurement noise. In order to prove the accuracy and robustness of the proposed RECKF-LQR based SAPF, a relative assessment has been performed employing a linear variant of the Kalman filter (KF). The whole performances of KF-LQR and the proposed RECKF-LQR based SAPF systems are investigated through the developed prototype employing dSPACE1104. The outcomes obtained reveal that the proposed RECKF-LQR approach delivers excellent performance in terms of dc voltage tracking, reference current tracking as well as current harmonics mitigation in the SAPF system.

References

1.Iqbal, F., Khan, M.T., and Siddiqui, A.S. (2018) Optimal placement of DG and DSTATCOM for loss reduction and voltage profile improvement. *Alexandria Engineering Journal*, **57** (2), 755–765.

2.Patjoshi, R.K., and Mahapatra, K. (2017) High-performance unified power quality conditioner using non-linear sliding mode and new switching dynamics control strategy. *IET Power Electronics*, **10** (8), 863–874.

3.Panigrahi, R., Subudhi, B., and Panda, P.C. (2015) A robust LQG servo control strategy of shunt-active power filter for power quality enhancement. *IEEE Transactions on Power Electronics*, **31** (4), 2860–2869.

4.Panigrahi, R., Subudhi, B., and Panda, P.C. (2014) Model predictive-based shunt active power filter with a new reference current estimation strategy. *IET Power Electronics*, **8** (2), 221–233.

5.Patjoshi, R.K., and Mahapatra, K. (2016) High-performance unified power quality conditioner using command generator tracker-based direct adaptive control strategy. *IET Power Electronics*, **9** (6), 1267–1278.

6.Yavari, M., Edjtahed, S.H., and Taher, S.A. (2018) A non-linear controller design for UPQC in distribution systems. *Alexandria engineering journal*, **57** (4), 3387–3404.

7.Patjoshi, R.K., and Mahapatra, K. (2016) Resistive optimization with enhanced PLL based nonlinear variable gain fuzzy hysteresis control strategy for unified power quality conditioner. *International Journal of Electrical Power & Energy Systems*, **83**, 352–363.

8.Popescu, M., Bitoleanu, A., and Suru, V. (2012) A DSP-based implementation of the pq theory in active power filtering under nonideal voltage conditions. *IEEE Transactions on Industrial Informatics*, **9** (2), 880–889.

9.Patjoshi, R.K., and Mahapatra, K.K. (2013) Performance comparison of direct and indirect current control techniques applied to a sliding mode based shunt active power filter. *2013 Annual IEEE India Conference (INDICON)*, 1–5.

10.Kumar, R., Singh, B., Shahani, D.T., and Jain, C. (2016) Dual-tree complex wavelet transform-based control algorithm for power quality improvement in a distribution system. *IEEE transactions on industrial electronics*, **64** (1), 764–772.

11.Dirik, H., and Özdemir, M. (2014) New extraction method for active, reactive and individual harmonic components from distorted current signal. *IET Generation, Transmission & Distribution*, **8** (11), 1767–1777.

12.Huang, C.-H., Lee, C.-H., Shih, K.-J., and Wang, Y.-J. (2010) A robust technique for frequency estimation of distorted signals in power systems. *IEEE Transactions on Instrumentation and Measurement*, **59** (8), 2026–2036.

13.Dash, P.K., Jena, R.K., Panda, G., and Routray, A. (2000) An extended complex Kalman filter for frequency measurement of distorted signals. *IEEE Transactions on Instrumentation and Measurement*, **49** (4), 746–753.

14.Panigrahi, R., and Subudhi, B. (2016) Performance Enhancement of Shunt Active Power Filter H-infinity Control Strategy. *IEEE Transactions on Power Electronics*, **32** (4), 2622–2630.

15.Panigrahi, R., Panda, P.C., and Subudhi, B. (2014) A robust extended complex Kalman filter and sliding-mode control based shunt active power filter. *Electric Power Components and Systems*, **42** (5), 520–532.

16.Kwan, K.H., So, P.L., and Chu, Y.C. (2012) An output regulation-based unified power quality conditioner with Kalman filters. *IEEE Transactions on Industrial Electronics*, **59** (11), 4248–4262.

17.Costanza, V., Rivadeneira, P.S., and Munera, J.A.G. (2016) Numerical treatment of the bounded-control LQR problem by updating the final phase

value. *IEEE Latin America Transactions*, **14** (6), 2687–2692.

18.Bhawal, C., and Pal, D. (2019) Almost Every Single-Input LQR Optimal Control Problem Admits a PD Feedback Solution. *IEEE Control Systems Letters*, **3** (2), 452–457.